Self-organization in Kerr-cavity-soliton formation in parametric frequency combs

Y. Henry Wen, Michael R. E. Lamont, Steven H. Strogatz, and Alexander L. Gaeta

Phys. Rev. A **94**, 063843 — Published 19 December 2016

DOI: 10.1103/PhysRevA.94.063843

Self-organization in Kerr cavity soliton formation in parametric frequency combs

Y. Henry Wen,[1,2,*] Michael R. E. Lamont,[1] Steven H. Strogatz,[3] and Alexander L. Gaeta[4]

[1] *School of Applied & Engineering Physics, Cornell University, Ithaca, NY 14853, USA*
[2] *Clarendon Laboratory, University of Oxford, Parks Road, Oxford OX1 3PU, UK*
[3] *Center for Applied Mathematics, Cornell University, Ithaca, NY 14853, USA*
[4] *Department of Applied Physics and Applied Mathematics, Columbia University, New York, New York 10027, USA*

We show that self-organization and synchronization underlie Kerr cavity soliton formation in parametric frequency combs. By reducing the Lugiato-Lefever equation to a set of phase equations, we find that self-organization arises from a two-stage process via pump-degenerate and pump-nondegenerate four-wave mixing. The reduced phase equations are akin to the Kuramoto model of coupled oscillators and intuitively explain the origin of the pump phase offset, predict anti-symmetrization of the intracavity field before phase synchronization, and clarify the role of chaos in Kerr cavity soliton formation in parametric combs.

PACS numbers: 42.82.Et, 03.65.Xp, 42.65.Pc

I. INTRODUCTION

Coupled oscillators with slightly different natural frequencies can self-organize to a synchronized state. This phenomenon appears throughout biology, chemistry, neuroscience, and physics [1, 2]. Examples include power grid networks, neural networks, chemical oscillators, and arrays of Josephson junctions and semiconductor lasers [3–7]. Self-organization in such systems has been modelled with a set of mean-field equations proposed by Kuramoto:

$$\dot{\phi}_p = \omega_p + (\kappa/N)\sum_m^N \sin(\phi_m - \phi_p), \tag{1}$$

where $\phi_p(t)$ is the phase of the p^{th} oscillator, ω_p is its natural frequency, and κ is the coupling strength [1, 2]. This model can be recast in an order-parameter formulation, where an average phase $\psi(t)$ and a coherence $R(t)$ are defined via

$$Re^{i\psi} = \frac{1}{N}\sum_m^N e^{i\phi_m}, \tag{2}$$

and visualized in Fig. (1a,b). The Kuramoto model then reduces to

$$\dot{\phi}_p = \omega_p + \kappa R(t)\sin(\psi - \phi_p). \tag{3}$$

Viewed in this way, the ϕ_p's are no longer coupled to each other, but only to the average phase ψ. Moreover the effective coupling strength is proportional to the coherence $R(t)$. This proportionality between coupling and coherence creates a positive feedback which, above a critical κ, triggers a transition in which a macroscopic fraction of the oscillators' frequencies spontaneously synchronizes to a single frequency.

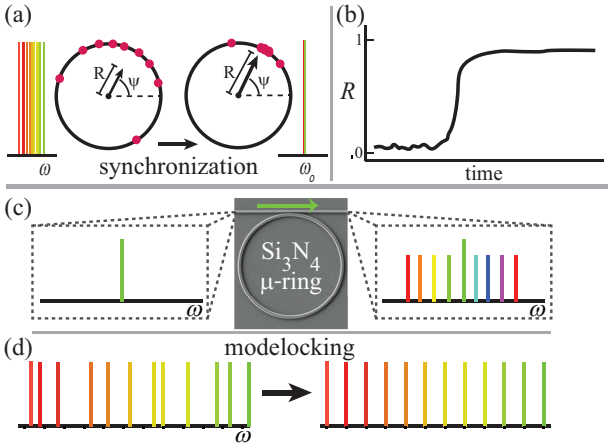

FIG. 1. (a) Synchronization of oscillators with distinct natural frequencies to a phase-locked state with a single frequency. A large fraction of the oscillator phases lock to ψ, the average phase. (b) Synchronization transition of the coherence R. (c) Broadband frequency comb-generation via continous-wave pumped four-wave mixing in silicon nitride micro-rings. (d) Modelocking of the cavity modes results in equidistant frequency spacings.

In optics an alternative form of phase locking can occur in lasers and parametric oscillators between a large collection of cavity modes with nearly equally spaced frequencies. In these systems the nearest-neighbor mode spacing varies due to dispersion within the cavity. Sufficient nonlinearity within the cavity can cause spontaneous modelocking such that the mode spacings become identical (Fig. 1c,d). This behavior has been studied in ultrashort pulse generation in lasers [8–11] and in microresonator-based four-wave mixing (FWM) parametric oscillators [13, 15–18] where they are known as temporal dissipative Kerr cavity solitons. Such oscillators have applications in optical information storage and processing [19], broadband frequency combs [20],

* Corresponding author: henry.wen@physics.ox.ac.uk

optical spectroscopy, and frequency metrology [21–23].

While several theoretical [24–26] and experimental studies [27, 28] have elucidated the phase dynamics of the initial formation of parametric combs, no corresponding analysis exists for soliton modelocking. It has been noted that passive modelocking in lasers is thermodynamically equivalent to a first-order phase transition, though no treatment of phase dynamics is provided [29]. Furthermore, although Kerr-based parametric frequency combs have been suggested as the most fundamental example of self-organization in nonlinear optics [19, 30], no direct connection has been made to the concepts of synchronization and self-organization.

In this paper, we reduce the Lugiato-Lefever equation (LLE) to a set of phase equations. These equations display self-organized dynamics akin to those in the Kuramoto model, including meaningful order parameters and coherence-coupling feedback, which we show underlies the formation of Kerr cavity solitons. These equations capture much of dynamics of the LLE despite neglecting the amplitude dynamics of the non-pump modes. They predict that this self-organization arises from a two-stage process. First the pump-degenerate (PD)-FWM processes anti-symmetrize the phases of symmetric modes about the pump mode, which constrains the phase averages of the symmetric modes. This in turn allows the pump-nondegenerate (PND)-FWM processes to synchronize the phase differences through a coherence-coupling feedback mechanism. The equations also predict an offset of the pump phase from the rest of the modal phase profile in the cavity soliton state. This offset cannot be accounted for by the detuning of the pump field alone; rather it stems from the need for a sine-like restoring force on phase averages. We compare the evolution of the phase equations to that of the full LLE system and observe a strong correspondence between them, indicating that the phase model captures the dynamics leading to the formation of cavity solitons. These observations provide novel insight into a highly important problem in laser and nonlinear optical physics, which is to understand the way in which many modes participate in the formation of localized structures.

The paper is organized as follows. In section II we reduce the Lugiato-Lefever Equation into a set of dynamical phase and amplitude equations by taking a spectral-modal plane wave ansatz, assuming a slowly varying modal envelope approximation and neglecting the spectral mode amplitude dynamics. In section III we consider the case of a single-mode parametric pumping which allows us to further reduce the dynamical phase equation into two coupled equations that describe the dynamics of the phase average and phase difference, respectively, of symmetric pairs of modes about the pump mode. We call these the Kerr phase equations (KPE), and from these equations we are able to draw several key insights into the cavity soliton formation process. In section IV we compare the temporal dynamics of the KPE with the LLE and show strong qualitative similarity between the KPE and the LLE.

II. REDUCTION OF THE LLE INTO PHASE AND AMPLITUDE EQUATIONS

The governing equation of modelocked parametric frequency combs is the LLE (a damped, driven nonlinear Schrödinger equation inside a cavity) with periodic boundary conditions [31]:

$$T_r\frac{\partial A}{\partial t} = A_{in} - \big[\frac{\alpha}{2} + i\delta_o\big]A + iL\Big[\sum_{k\geq 1}^{3}\frac{\beta_k}{k!}\left(i\frac{\partial}{\partial \tau}\right)^k + \gamma|A|^2\Big]A, \tag{4}$$

where A is the intra-cavity field, t and τ are the slow and fast times of the system, A_{in} is the pump field coupled into the cavity at frequency $\omega_{\delta 0} = \omega_0 + \delta_o/T_r$ where δ_o/T_r is the detuning of the pump field from the center of the cavity resonance, β_k are dispersion coefficients, γ is the nonlinear coefficient, α is the total linear loss per round trip of the cavity of length L, and $T_r = L/v_g$ is the round trip time. We consider the intra-cavity field as a sum of the discrete cavity modes and define a phase $\phi_p^{'}(t)$ for each mode at the frequency corresponding to the equidistant comb defined by the detuned pump field such that $A(t,\tau) = \sum_p^{N+1} A_p \exp i(\omega_p - \omega_{\delta o})t - i(\Omega_p - \Omega_0)\tau e^{i\phi_p^{'}(t)}$. By letting the pump mode index $p_0 = 0$, where N is even and $-N/2 \leq p \leq N/2$, the slow and fast frequencies of the field become $\omega_p = 2\pi v_g p/L + \omega_{\delta o}$ and $\Omega_p = 2\pi v_g p/L + \Omega_{\delta o}$. For a sufficiently strong pump field $A_{in}(t,\tau) = A_0 e^{i(\phi_0 + \delta_o t)}$ with appropriate cavity detuning δ_o and constant phase ϕ_0, a broadband comb of frequencies is generated near the modes of the cavity (Fig.1c). After an initial build-up period, the amplitudes of the cavity modes reach a near steady state. Thus, we are able to neglect the amplitude variations of the modes and consider only the phases. By using normalized dispersion coefficients $\xi_k = (2\pi v_g/L)^k v_g \beta_k$, we transform into a generalized form of the LLE[32]:

$$\frac{\partial A}{\partial t} = i\sum_{k\geq 1}^{3}\frac{\xi_k}{k!}\left(i\frac{\partial}{\partial \eta}\right)^k A - i\Gamma|A|^2 A - \frac{\Delta\omega_o}{2}A \tag{5}$$

$$A(t,\eta) = \sum_p^N A_p \exp i\Big[(\omega_p - \omega_{\delta o})t - (p - p_o)\eta + \phi_p^{'}(t)\Big], \tag{6}$$

where η is the angle around the circumference of the cavity and ξ's correspond to the dispersion coefficients. ω_o and p_o are the frequency and the mode number of the pumped mode, and $\Gamma = \gamma L/T_r$ is the four-wave mixing gain coefficient.

By inserting the modal ansatz into the general LLE and following the derivation detailed in Appendix A we

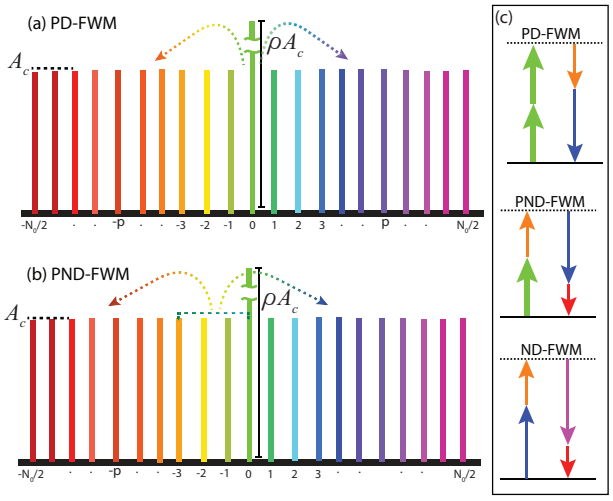

FIG. 2. Scheme for (a) pump-degenerate and (b) pump-nondegenerate four-wave mixing. The amplitude of the central pump-mode is ρ times stronger than the non-pump modes.(d) Energy diagrams for the PD-FWM, PND-FWM and nondegenerate (ND)-FWM processes.

obtain the following pair of equations for the phases and amplitudes of comb modes,

$$\dot{\phi}_p = \sum_{k\geq 2}^{3} \frac{\xi_k}{k!}(p)^k - \Gamma \sum_{lmn}^{N} A_{lp}^2 \delta_{mp}^{ln} \cos(\phi_{mp}^{ln}) \qquad (7)$$

$$\dot{A}_p = -\frac{\Delta\omega_o}{2} - \Gamma \sum_{lmn}^{N} A_{lp}^2 \delta_{mp}^{ln} \sin(\phi_{mp}^{ln}), \qquad (8)$$

where $A_{lp} = \sqrt{A_l A_m A_n / A_p}$, $\phi_{mp}^{ln}(t) = \phi_l(t) - \phi_m(t) + \phi_n(t) - \phi_p(t)$ and δ_{mp}^{ln} is a generalized Kronecker delta that is unity when $l - m + n - p = 0$ and zero otherwise. This set of equations is numerically identical to the LLE. However, it does explicitly show the dependence of the phase of each mode on the phases and amplitudes of other modes. Equation 7 also shows structural similarities to the Kuramoto model with phase dynamics defined as an interplay between frequency disorder terms, arising from dispersion, and a coupling arising from the Kerr nonlinearity. However, the Kerr coupling term, with four-phase interactions, is significantly more complicated than the two-phase interactions of the Kuramoto model.

III. THE KERR PHASE EQUATIONS: THE PHASE-AVERAGE AND PHASE-DIFFERENCE EQUATIONS

In the rest of the paper we focus on the dynamical phase equation (Eq.7), since we are interested in the phase dynamics of the cavity soliton formation process. In the following section we reduce this equation, in the case of single frequency parametric pumping, into two coupled equations for the *phase average* and *phase difference* of symmetric modes about the pump. We first consider the role of the amplitudes on the terms in the coupling term. If all the amplitudes are identical (i.e. $A_l = A_m = A_n = A_p = A_c$), then Eq.7 has no globally stable solution. The cosine coupling function pulls its argument towards a value of $-\pi/2$. However, this criterion cannot be satisfied by all energetically appropriate combination of phases simultaneously. So it is apparent that a comb with all modes having equal amplitude can not be stable.

Under conditions of comb generation, the pump field is typically several orders of magnitude stronger than the non-pump modes. We assume all non-pump modes, ranging from $-N_o/2$ to $N_o/2$, have the same amplitude (A_c). The pump mode then has amplitude $A_0 = \rho A_c$ as shown in Fig. 2, with ρ having values typically from 10-100. This allows the decomposition of the Kerr coupling term and its constituent FWM process via the amplitude coefficients A_{lp}^2 into classes of terms with relative strengths ρ^2, ρ, 1, and ρ^{-1}. In our analysis we keep only the strongest FWM processes, which scale as ρ^2 and ρ. The terms that scale as ρ^2 are a result of the PD-FWM processes, where two pump photons are annihilated to create a photon pair at modes symmetric about the pump mode (Fig.2a). The terms that scale as ρ are due to the PND-FWM processes, in which one pump photon and one comb photon are annihilated and create two photons at the energetically appropriate modes (Fig.2b). This decomposition leads to the following Kerr coupling terms:

$$\overbrace{\Gamma A_c^2 \rho^2 \cos\left[2\phi_0 - (\phi_p + \phi_{-p})\right]}^{PD-FWM} - \underbrace{\Gamma A_c^2 \rho \sum_{m=-N_o/2}^{N_o/2} \cos\left[\phi_0 + (\phi_m - \phi_{m-p}) - \phi_p\right]}_{PND-FWM}. \qquad (9)$$

There is only one PD-FWM term, and it has in its argument the value $(\phi_p + \phi_{-p})$, which corresponds to a phase average of the p^{th} modes symmetric about the pump.

The presence of the phase average term in the Kerr coupling term suggests that the natural variables to describe the system are not the individual phases but are rather the phase average and difference for pairs of modes symmetric about the pump mode, that is, $\bar{\phi}_p = (\phi_p + \phi_{-p})/2$ and $\theta_p = (\phi_p - \phi_{-p})/2p$, respectively. Additionally, since the PD-FWM term is ρ times stronger than the PND-FWM term, and the PND-FWM term is close to zero due to random initial phases, the PD-FWM dominates the initial dynamics, with the cosine having the effect of anti-symmetrizing the phases of symmetric modes such that $(\phi_p - \phi_o) \approx -(\phi_{-p} - \phi_o)$. Following the derivation detailed in Appendix B we obtain the following set of equations for the phase average and phase difference of symmetric pairs of modes, which

together comprise the *Kerr phase equations*(KPE),

$$\dot{\bar{\phi}}_p = \frac{\xi_2}{2}p^2 - 2\Gamma\rho^2 A_c^2 \cos[2(\phi_0 - \bar{\phi}_p)] - \Gamma\rho A_c^2 N_o R(t)\cos(\phi_0 - \bar{\phi}_p)\cos[p(\theta_p - \theta_o)], \tag{10}$$

$$\dot{\theta}_p = \frac{\xi_3}{3}p^2 - \frac{2\Gamma\rho A_c^2 N_o}{p}R(t)\sin(\phi_0 - \bar{\phi}_p)\sin[p(\theta_p - \theta_o)], \tag{11}$$

where θ_o is the normalized average phase difference, analogous to ψ in the Kuramoto model (Eq. 3). It corresponds to the slope of the phase profile which yields a temporal translation of the pulse profile along the cavity length. The coherence $R(t)$ measures the extent to which the phase differences θ_m align to their average θ_o, and are given by,

$$\theta_o(t) = \frac{8}{N_o^2}\sum_{m=1}^{N_o/2} m\theta_m, \tag{12}$$

$$R(t) = \frac{2}{N_o}\left|\sum_{m=1}^{N_o/2}\exp im(\theta_m - \theta_0)\right|, \tag{13}$$

The triple sum reduces to a single sum, and the phase-average and phase-difference parameters are separable due to the phase anti-symmetry induced by the PD-FWM term.

IV. CAVITY SOLITON FORMATION IN THE KERR PHASE EQUATIONS

In this section we analyze the dynamics of cavity soliton formation as described by the KPE and compare these results to those of the full LLE. Since the KPE is a set of reduced phase equations for which the amplitude variations have been neglected, we should seek qualitative agreement between the two models and intuitive understanding of the dynamics via the analytical nature of the KPE.

We begin by considering the evolution of the KPE system starting from a random phase profile. Since the PD-FWM term scales as ρ^2, it initially dominates the dynamics. Its presence in the phase-average equation (Eq. 10) tends to anti-symmetrize the phase profile about the pump phase ϕ_0. The PND-FWM terms do not initially play a role since the coherence $R(t)$ is zero (due to the initially random phases), $\sin(\phi_0 - \bar{\phi}_p)$ is typically zero as well, and since they are inherently ρ times smaller than the PD-FWM terms. Once anti-symmetrization of the phases occurs the $\sin(\phi_0 - \bar{\phi}_p)$ factor become non-zero and the coherence builds up via in the phase-difference equation. This self-organization results in a near-linear spectral phase profile, which is consistent with evolution to a well-defined pulse (i.e. a cavity soliton) as predicted by the LLE model. Thus, the initial dynamics leading to synchronization and soliton formation consists of the following two stages: the PD-FWM term entrains the phase averages to a fixed input phase; whereas the PND-FWM term uses coherence-coupling feedback to self-organize the system around a non-fixed normalized average phase difference.

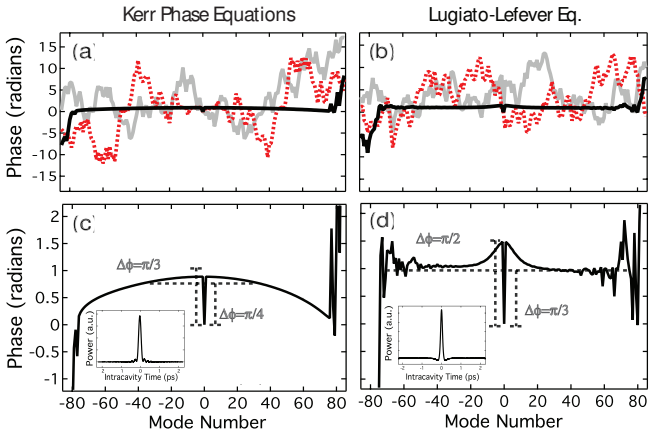

FIG. 3. (a,b) Three stages of evolution of the intra-cavity field predicted by (a) the KPE and (b) the LLE. Solid grey curves represent the initial random phase profile. Dotted red curves show the phase evolution after 370 (KPE) or 308 (LLE) round trips; both phase profiles depict the anti-symmetrization of the spectral phase due to the pump degenerate FWM processes. Black curves show the final phase profile after 3394 round trips (both models). The phases have become synchronized by the pump non-degenerate terms. Note the slight offset of the pump phase from the phases of the other cavity modes. (c,d) The final spectral phase profiles of the KPE and LLE systems deviate from a pure linear profile, including the pump phase offsets. (insets) Temporal pulse shapes of the KPE and LLE.

We perform numerical simulations of the temporal evolution of the KPE and the full LLE systems using parameters presented in [35] and verify the self-organization route to cavity soliton formation. For both models, Figs. 3(a,b) show the predicted two-stage progression from an initially random phase profile to an anti-symmetric profile and then to full synchrony. A notable feature of the LLE cavity soliton phase profile is a static offset of the pump phase from the rest of the phase profile. This offset cannot be explained by time-constant phase shifts such as the pump field detuning, self-phase modulation, or cross-phase modulation.

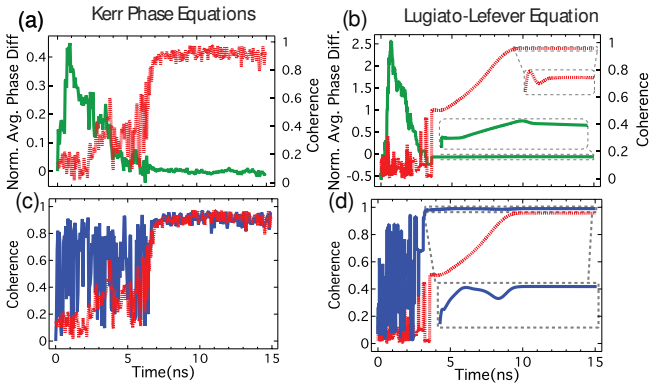

FIG. 4. Coherence R (red-dotted) and normalized average phase difference θ_o (green) for the (a) Kerr Phase Equations (KPE) and the (b) Lugiato-Lefever Equation (LLE). Both systems show an abrupt transition to a stable phase-synchronized state. Coherence R (red-dotted) and phase symmetry R_{asym} (blue) for the (c) KPE and (d) LLE.

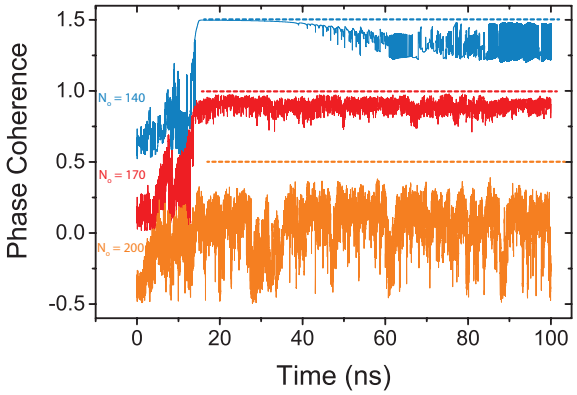

FIG. 5. Time evolution of the coherence for the KPE for three values of N_o= 140, 170, 200. The equations are only stable for $185 > N_o > 155$, which is consistent with the soliton condition of the LLE.

Rather it results from phase matching conditions of the dominant FWM processes identified above. It can also be understood from the KPE system: In order for the PD-FWM term to act as a restoring force on the phase averages as in the Kuramoto model, it must have a sinusoidal, rather than co-sinusoidal, dependence on the phase averages. We compare in detail the spectral phase profiles in Fig. 3(c,d). Both systems stabilize to a broadband phase-locked state with an offset of the pump phase from the rest of the phase profile. Due to the factor of 2 in the argument of the PD-FWM cosine term, this offset should be $0 < \Delta\phi < \pi/2$ and centered at $\pi/4$ for the term to have a significant sine-like contribution. Both the KPE and the LLE predict pump phase offsets within these bounds. The LLE system has a slightly larger pump phase offset due to self-phase and pump-induced cross-phase modulation effects neglected in the KPE. The insets in Fig. 3(c,d) confirm that the broadband phase-locked state gives a solitary pulse in the time domain. The exact pulse shape for the KPE is not particularly meaningful since the modes have equal amplitude, yielding a sinc-like pulse without a CW background. This is, to our knowledge, the first explanation of the pump phase offset of the cavity soliton-modelocked states in a Kerr comb.

The evolution of the order parameters further validates our claims that 1) the amplitude dynamics of the comb are negligible and 2) the PD-FWM processes anti-symmetrize the phases prior to the onset of phase synchronization. Figure 4(a,b) compares how $R(t)$ and $\theta_o(t)$ evolve in the KPE and LLE systems. Despite slight quantitative differences, both systems exhibit abrupt transitions to an ordered state, as indicated by the sharp rise and subsequent stabilization of the coherence R. Likewise, $\theta_o(t)$ behaves similarly in both systems; after an initial rapid increase, it declines and stabilizes at a constant value. Closer inspection of the two parameters (insets) reveals relaxation behavior on the order of 1 ns, close to the cavity lifetime of 1.42 ns. The remarkable quantitative similarity of dynamics indicates that the cavity soliton formation process is truly dominated by phase rather than amplitude dynamics.

Next we consider the parameter $R_{\text{asym}} = \frac{2}{N_o}\left|\sum_{m=1}^{N_o/2} e^{i(\bar{\phi}_m - \phi_0)}\right|$, which quantifies the extent to which the phase profile is anti-symmetric about the pump phase and is equivalent to a coherence of the phase averages. Figure 4(c,d) shows that in both systems, phase anti-symmetry occurs before coherence is achieved, and the coherence cannot grow until the phase anti-symmetry has reached a high value. This confirms our initial prediction that the PD-FWM term must anti-symmetrize the phase profile before the PND-FWM term can synchronize the phases to a near linear profile. These dynamics are only observed in cavity soliton formation, not in the Turing pattern or chaotic states. Furthermore, the phase symmetry does not fully stabilize until the coherence has reached a high value, and in turn, the coherence does not stabilize until the phase symmetry has fully stabilized. These results illustrate the necessity of phase anti-symmetrization to precede phase synchronization in cavity soliton formation and the complex interplay between phase symmetry and phase coherence. We further find that synchronization in the KPE is stable only for $185 > N_0 > 155$ as shown in Fig. 5. Choosing the most stable number $N_0 = 170$ results in synchronization of 152 modes, in close correspondence to the LLE where 155 modes are locked. This indicates that the KPE synchronization bandwidth depends on the balance of disorder and coupling and is not simply constrained to N or N_o.

Passage through a chaotic state has been suggested as necessary for cavity soliton modelocking to occur [35, 36]. The correspondence between Fig. 4(a,c) and (b,d) suggests that the role of the chaotic stage is to randomize the phase profile, thereby preventing Turing

pattern and mini-comb-related FWM processes from dominating the phase matching of the comb [25, 37]. Turing states and the associated mini-combs have phase profiles that lack global symmetry about the pump phase and thus cannot directly enter into a cavity soliton state. However, some parameter regimes of the KPE yield phase profiles with multiple phase-offset modes and phase-steps, similar to states measured by Del'Haye *et al.* [27], and are the subject of ongoing work. In saturable-absorption-based modelocked lasers the coupling term in Eq. (A7) will include a significant sine component, and phase synchronization is possible without a coherent pump field. Given the generality of the root equation of the LLE, which is the complex Ginzburg-Landau equation, this synchronization model may be applicable to the phase transition dynamics in a wide range of nonlinear dissipative systems.

Appendix A: Reduction of the LLE into phase and amplitude equations

In Appendix A we detail the derivation that reduces the LLE equation with discrete modes (Eqs. 5, 6) into a pair of dynamical equations for the amplitude and phases of the modes (Eqs. 8, 7). Since the modes represented in Eq. 6 exist on a nearly equidistant grid of frequencies, all of the phase dynamics of each mode can be parametrized by the factor $\phi_p^{'}(t)$. We can transform into the group velocity frame by using $\eta \rightarrow \eta - \xi_1 t$. By expanding the modal frequencies explicitly in terms of the mode number and dispersion ($\omega_p \approx \omega_{p_o} + \xi_1(p-p_o) + \frac{1}{2}\xi_2(p-p_o)^2$)and letting $p_o = 0$ we obtain $A(t,\eta) = \sum_p^N a_p \exp i\left[\frac{\xi_2}{2}p^2 t - p\eta + \phi_p^{'}(t)\right]$. Furthermore, we can include dispersion effects into the phase factor without losing generality, $\phi_p^{'}(t) + \frac{1}{2}\xi_2 p^2 t + \frac{1}{6}\xi_3 p^3 t \rightarrow \phi_p(t)$. Injecting the field into the left hand side (LHS) of the LLE we obtain,

$$\frac{\partial A}{\partial t} = \sum_p^N A_p \exp i\left[p\eta + \phi_p(t)\right]\left(\dot{A}_p + i\dot{\phi}_p(t)\right) \quad \text{(A1)}$$

For the right hand side (RHS) of Eq. (5) we examine each term. The dispersive terms:

$$i\sum_{k\geq 2}^{3}\frac{\xi_k}{k!}\left(i\frac{\partial}{\partial\eta}\right)^k A = -i\sum_p^N A_p \exp\left(i\phi_p(t)\right)\sum_{k\geq 2}^{3}\frac{\xi_k}{k!}\left(i\frac{\partial}{\partial\eta}\right)^k \exp\left(-ip\eta\right) = iA\sum_{k\geq 2}^{3}\frac{\xi_k}{k!}p^k \quad \text{(A2)}$$

and results in a term linear in the field A. The Kerr term becomes:

$$i\Gamma|A|^2 A = i\Gamma\sum_{l,m,n}^{N}\frac{A_l A_m A_n}{A_p}\exp i\left[\phi_l - \phi_m + \phi_n\right]. \quad \text{(A3)}$$

The loss term is a scalar multiple of the field, that is, $-\frac{\Delta\omega_o}{2}A$. Next we recombine the LHS and RHS of Eq. 5 and factor out the quantity $iA(t)$ from both sides of the equation, which results in the following:

$$\dot{\phi}_p(t) - i\dot{A}_p(t) = i\frac{\Delta\omega_o}{2} + \sum_{k\geq 2}^{3}\frac{\xi_k}{k!}p^k - \frac{i\Gamma|A|^2 A}{A_p\exp\left[i\phi_p(t)\right]}. \quad \text{(A4)}$$

The Kerr term (i.e., the final term in Eq. (A4)) can be further simplified:

$$= i\Gamma\sum_{l,m,n}^{N}A_{lp}^2\exp i[\phi_l(t) - \phi_m(t) + \phi_n(t) - \phi_p(t)] \quad \text{(A5)}$$

where $A_{lp} = \sqrt{A_l A_m A_n / A_p}$ and where energy conservation constrains the indices to the condition $l-m+n-p = 0$. Putting this back in Eq. (5) we obtain,

$$\dot{\phi}_p(t) - i\dot{A}_p(t) = i\frac{\Delta\omega_o}{2} + \sum_{k\geq 2}^{3}\frac{\xi_k}{k!}(q)^k - \Gamma\sum_{l,m,n}^{N}\delta_{mp}^{ln}A_{lp}^2\exp i\left[\phi_{mp}^{ln}(t)\right], \quad \text{(A6)}$$

where $\phi_{mp}^{ln}(t) = \phi_l(t) - \phi_m(t) + \phi_n(t) - \phi_p(t)$ and δ_{mp}^{ln} is a generalized Kronecker delta that is unity when $(l+n) = (m+p)$ and zero otherwise. We separate the real and imaginary parts of the equation to obtain the following pair of equations for the phases and amplitudes, respectively,

$$\dot{\phi}_p = \sum_{k\geq 2}^{3}\frac{\xi_k}{k!}(p)^k - \Gamma\sum_{lmn}^{N}A_{lp}^2\delta_{mp}^{ln}\cos(\phi_{mp}^{ln}) \quad \text{(A7)}$$

$$\dot{A}_p = -\frac{\Delta\omega_o}{2} - \Gamma\sum_{lmn}^{N}A_{lp}^2\delta_{mp}^{ln}\sin(\phi_{mp}^{ln}). \quad \text{(A8)}$$

Appendix B: Derivation of The Kerr phase equations

In Appendix B we detail the derivation that transforms the dynamical phase equation (Eq. 7) into the Kerr phase equations (Eqs. 10, 11), a pair of coupled equations for the phase averages and phase differences of symmetric

pairs of modes.

$$\dot{\bar{\phi}}_p = \frac{\xi_2}{2}p^2 - 2\Gamma A_c^2\rho^2\cos[2(\phi_0 - \bar{\phi}_p)] - 2\Gamma A_c^2\rho\sum_{m=1}^{N_o/2}\big(\cos[\phi_0 + (\phi_m - \phi_{m-p}) - \phi_p] + \cos[\phi_0 + (\phi_{-m} - \phi_{p-m}) - \phi_{-p}]\big). \quad \text{(B1)}$$

Due to the frequency-symmetric nature of the phase average, this equation represents the "even" behavior of the system, which includes the second order dispersion, PD-FWM and the sum of the PND-FWM. PD-FWM is ρ times stronger than the PND-FWM, and the PND-FWM is initially zero due to random phases. Thus the PD-FWM dominates the initial dynamics, with the cosine having the effect of anti-symmetrizing the phases of symmetric modes such that $(\phi_p - \phi_o) \approx -(\phi_{-p} - \phi_o)$. A key feature of this term is that it predicts a phase offset of the pump from the rest of the phase profile by $\pi/4 < \Delta\phi_0 < \pi/2$, since such an offset is necessary to produce a sine-like coupling term that can compensate for dispersion and lead to synchronization. We define the phase difference of the p^{th} modes symmetric on either side of the pump as $p\theta_p = (\phi_p - \phi_{-p}))/2$. The resulting equation of motion is given by

$$p\dot{\theta}_p = \frac{\xi_3}{3}p^3 - 2\Gamma A_c^2\rho\sum_{m=1}^{N_o/2}\Big(\cos[\phi_0 + (\phi_m - \phi_{m-p}) - \phi_p] - \cos[\phi_0 + (\phi_{-m} - \phi_{p-m}) - \phi_{-p}]\Big). \quad \text{(B2)}$$

This equation contains the "odd" terms such as the third-order dispersion and the difference of the PND-FWM terms. The sum of the two cosine terms becomes

$$\begin{aligned}\cos\left[\phi_0 + (\phi_m - \phi_{m-p}) - \phi_p\right] &- \cos\left[\phi_0 + (\phi_{-m} - \phi_{p-m}) - \phi_{-p}\right] \\ &= -2\sin\left[p\left(\frac{\theta_{mp} - \theta_{-mp}}{2} + \theta_p\right)\right] \\ &\quad\times\sin\left[\phi_0 - p\left(\frac{\theta_{mp} + \theta_{-mp}}{2} - \bar{\phi}_p\right)\right], \quad \text{(B3)}\end{aligned}$$

where $\theta_{\pm mp} = \phi_{\pm m} - \phi_{\pm(m-p)}$. The same reduction applies to the PND-FWM term in the phase average equation except the corresponding angle addition formula must be use in place of the angle difference formula. We recall from the phase average equation that due to the anti-symmetrizing effect of the PD-FWM, $(\phi_p - \phi_o) \approx -(\phi_{-p} - \phi_o)$, thus $\theta_{-mp} = -\theta_{mp}$ and the equation for the phase average simplifies to

$$p\dot{\theta}_p = \frac{\xi_3}{3}p^3 + 2\Gamma A_c^2\rho\sin(\phi_0 - \bar{\phi}_p) \times\sum_{m=1}^{N_o/2}\sin[m\theta_m + (p-m)\theta_{p-m} + p\theta_p)], \quad \text{(B4)}$$

allowing the phase average dependence to be pulled out of the sum, such that the coupling term is now a sum over one index. It can now be written in the form of an order parameter, in close analogy to the Kuramoto model, via the following relations:

$$R(t)\exp ip(\theta_o - \theta_p) = \frac{2}{N_o}\sum_{m=1}^{N_o/2}\exp ip(\theta_m + \theta_{p-m} - \theta_p), \quad \text{(B5)}$$

$$\frac{1}{N}\sum_{m=1}^{N}\exp i(m\theta_m + (N-m)\theta_{N-m}) \approx \frac{1}{N}\left(\sum_{m=1}^{N}\exp i(m\theta_m)\right)^2. \quad \text{(B6)}$$

Equation B6 is an approximation valid in the limit of large N and a mono-modal distribution of phase differences. Thus we are able to define the mean phase difference $\theta_o(t)$ and the coherence $R(t)$:

$$\theta_o(t) = \frac{8}{N_o^2}\sum_{m=1}^{N_o/2}m\theta_m, \quad \text{(B7)}$$

$$R(t) = \frac{2}{N_o}\left|\sum_{m=1}^{N_o/2}\exp im(\theta_m - \theta_0)\right|, \quad \text{(B8)}$$

which allows us to fully define the Kerr Phase equations given by Eqs. 10 and 11.

The authors thank I. Kloumann, Y. Okawachi, R. Lau, M. Yu and K. Wiesenfeld for insightful discussions, and the Defense Advanced Research Projects Agency Quasar program and the Air Force Office of Scientific Research grants FA9550-12-1-0377 and FA9550-15-1-0303 for supporting this work. Research of SHS was supported in part by NSF Grants DMS-1513179 and CCF-1522054.

[1] Y. Kuramoto, Chemical Oscillations, Waves and Turbulence (Springer-Verlag, Berlin, 1984).

[2] S. H. Strogatz, Physica D **143,** 1 (2000).

[3] A. E. Motter *et al.*, Nature Phys. **9,** 191 (2013).
[4] T. Womelsdorf *et al.*, Science. **316,** 1069 (2007).
[5] I. Z. Kiss *et al.*, Science **296**, 5573 (2010).
[6] K. Wiesenfeld *et al.*, Phys. Rev. Lett. **76**, 404 (1996).
[7] G. Kozyreff *et al.*, Phys. Rev. Lett. **85**, 3809 (2000).
[8] H. A. Haus, IEEE Quant. Electr. **6**, 1173 (2000).
[9] F. X. Kartner, IEEE Quant. Electr. **2**, 540 (1996).
[10] S. Fauve and O. Thaul, Phys. Rev. Lett. **64**, 282 (1990).
[11] N. Akhmediev and A. Ankiewicz, Dissipative solitons: from optics to biology and medicine, (Springer 2008).
[12] P. Del'Haye *et al.*, Nature **450**, 1214 (2007).
[13] K. Saha *et al.*, Opt. Express **21**, 1335 (2013).
[14] C. Joshi *et al.*, Opt. Lett **41**, 2565 (2014).
[15] T. Herr *et al.*, Nat. Photon. **8**, 145 (2014).
[16] V. Brasch *et al.*, Science **351**, 357 (2016).
[17] X. Yi *et al.*, Optica **2**, 1078 (2015).
[18] X. Xue *et al.*, Nat. Photon. **9**, 594 (2015).
[19] F. Leo *et al.*, Nat. Photon. **4**, 471 (2010).
[20] Y. Okawachi *et al.*, Opt. Lett **36**, 3398 (2011).
[21] T. Udem *et al.*, Nature **416**, 233 (2002).
[22] P. Del'Haye *et al.*, Nat. Photon. **10**, 516 (2016).
[23] S. B. Papp *et al.*, Optica **1**, 10 (2014).
[24] Y. Chembo *et al.*, Phys. Rev. Lett. **104**, 103902 (2010).
[25] A. Coillet *et al.*, arXiv:**1401**.0930 (2014).
[26] W. Loh *et al.*, Phys. Rev. A **89**, 053810 (2014).
[27] P. Del'Haye *et al.*, Nat. Comm.**6** 5668 (2015).
[28] X. X. Xue *et al.*, arXiv:**1404**.2865 (2014).
[29] A. Gordon and B. Fischer, Phys. Rev. Lett. **89**, 103901 (2002).
[30] W. J. Firth and C. O. Weiss, Opt. Photon. News **13**, 54 (2002).
[31] S. Coen *et al.*, Opt. Lett. **38**, 37 (2013).
[32] Y. Chembo, C. Menyuk, Phys. Rev. A **87**, 053852 (2013)
[33] D. Gomila *et al.*, Physica D (2007) **227**, 70 (2007).
[34] P. Parra-Rivas *et al.*, Phys. Rev. A **89**, 043813 (2014).
[35] M. R. E. Lamont *et al.*, Opt. Lett. **38**, 3478 (2013).
[36] A. Coillet and Yanne Chembo, Chaos **24** 013113 (2014).
[37] T. Herr *et al.*, Nat. Photon. **6**, 480 (2012).